NOTICE CONCERNING COPYRIGHT RESTRICTIONS

RESISTIVITY STRUCTURE OF THE NORTHERN BASIN AND RANGE

Philip E. Wannamaker

Earth Science Laboratory/University of Utah Research Institute
420 Chipeta Way, Suite 120
Salt Lake City, Utah 84108

ABSTRACT

Trustworthy models of northern Basin and Range resistivity have been lacking mainly due to an inadequate regard for the effects of upper crustal three-dimensional (3D) inhomogeneities upon the surface electromagnetic measurements. While geomagnetic deep sounding (GDS) is relatively insensitive to upper crustal complexity, the ability of GDS to resolve structure of interest at greater depths is limited. The role of low-resistivity 3D structures near the surface has been documented most thoroughly for the magnetotelluric (MT) technique, although controlled-source electromagnetics (CSEM) using either grounded or ungrounded transmitters also is seriously complicated by inhomogeneities. The natural field methods of MT and GDS are preferred to CSEM for deep resistivity exploration due to the plane-wave nature of the source as well as to the availability of data at very low frequencies and of 2D and 3D modeling algorithms for treating upper crustal structure.

Magnetotelluric measurements in S.W. Utah have detected a low-resistivity layer from 35 to 65 km depth in the upper mantle that is proposed to reflect an accumulation of basaltic melt in peridotite. GDS experiments and various tectonic indicators suggest that this melt is controlled by adiabatic upwelling and fusion along the eastern margin of the northern Basin and Range. Similar GDS anomalies and extensional processes appear active in the western margin of this province, implying a similar resistivity structure. This would leave the northern Basin and Range interior of central Nevada as a comparatively quiescent region with an upper mantle seismic low-velocity zone whose melt interconnection, and commensurate low resistivity, remain fairly intact.

INTRODUCTION

The gains in knowledge of earth processes by investigations of electrical resistivity structure traditionally have been modest compared to those by other geoscientific methods. A major reason for this is that the electromagnetic (EM) measurements at the surface, from which one infers subsurface resistivity, in general are contaminated by complexity in the uppermost crust to a degree that is more extreme than for other geophysical techniques.

Through the course of this paper, I will examine the pitfalls in the interpretation of EM measurements in tectonically active environments, review previous surveys of resistivity structure in the northern Basin and Range, and propose a model for the Late Cenozoic evolution of deep resistivity structure and physiochemical conditions throughout the northern Basin and Range.

RESISTIVITY SURVEYS IN THE NORTHERN BASIN AND RANGE

Several key surveys of northern Basin and Range resistivity structure will be studied in this section (see Figure 1). Methods utilizing

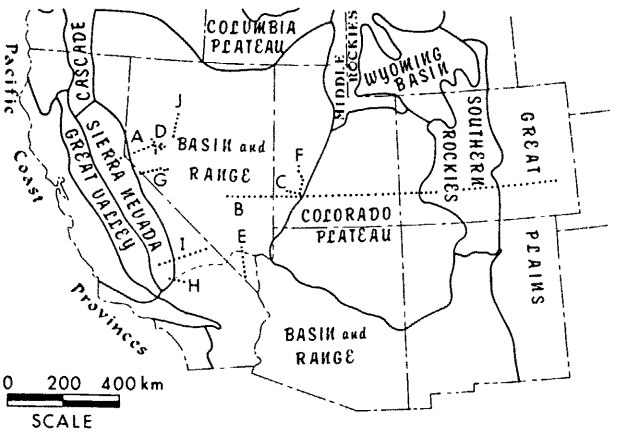

Figure 1. Physiographic provinces of the south western United States, modified from Stewart (1978). Dashed line separates Great Basin from the southern Basin and Range (Eaton, 1982). Locations are plotted for resistivity surveys discussed in text: A, Schmucker (1970); B, Porath (1971); C, MT survey at the Roosevelt Hot Springs, this paper; D, Stanley et al., 1976; E, Keller, 1971; F, Petrick et al., 1981; G, Lienert and Bennett, 1977; H, Lienert, 1979; I, Towle, 1980; J, Wilt et al., 1982.

either natural or artificial sources of EM fields have been applied. Principles of the techniques will not be reviewed here; the reader is referred to the literature cited for this purpose. I will, however, emphasize the effects on EM observations of the upper crustal three-dimensional (3D) heterogeneity so prevalent in the northern Basin and Range.

Geomagnetic Deep Sounding

Geomagnetic deep sounding (GDS), which makes use of natural magnetic field temporal variations, is less affected by upper crustal complexity than are the other EM methods I cover. The analysis of Wannamaker et al. (1983) can be extended easily to show that the secondary magnetic field transfer functions of GDS (Schmucker, 1970) are band-limited in frequency, with relatively small-scale, shallow structure like graben sediments responding over a frequency range which is higher than that of the deep regional resistivity structure of interest approximately as the square of the geometric scale factor distinguishing the two classes of structure. However, details of the separation depend on the layered host for the structures (Wannamaker et al., 1983). This separation of responses in frequency enables discrimination against surface inhomogeneity. Nevertheless, the response of the deep structure one seeks may itself be complicated; use of relatively simple 1D or 2D interpretation algorithms likely will yield models that are only qualitatively correct.

Pioneering measurements by Schmucker (1970) established geomagnetic anomalies indicating conductive upwellings beneath the Rio Grande Rift and the northwestern Basin and Range. Concerning the latter area, Schmucker places the conductive mass at a depth of 40 km in the upper mantle (Figure 2).

Much of what we know about the deep electrical resistivity of the northern Basin and Range and the Colorado Plateau is the result of geomagnetic temporal variations observed by Reitzel et al. (1970). Three components of magnetic field were recorded at periods from 20 to 200 minutes along four E-W profiles about 150 km apart, with station spacings averaging about 120 km. Porath et al. (1970) and Porath and Gough (1971) showed that anomalies in vertical and E-W horizontal fields were of internal origin (see Figure 3), with the external fields varying smoothly over the recording array. This behavior of the external fields severely limits the ability of GDS to resolve horizontal resistivity layering (Schmucker, 1970).

From these estimates of normalized anomalous fields, Porath (1971) presented a preferred, two-dimensional resistivity model, also shown in Figure 3, with a 2 Ω-m layer of varying thickness from the northern Basin and Range to the Great Plains, and with superimposed conductive ridges beneath the Wasatch Fault Belt and the Southern Rocky Mountains. This model was correlated with seismic LVZ estimates. Gough (1983) has reaffirmed the model of Porath (1971) and proposed that the conductive ridges in the upper mantle beneath western Utah and the southern Rocky Mountains reflect zones of partial melting. However, the intrinsic values of depth and resistivity are not well resolved (ibid.), especially given the assumption of purely 2D geometry. The secondary field amplitudes diminish to the south, and so presumably does the anomalous resistivity structure, but the features in Figure 3 appear to continue into northwesternmost Arizona.

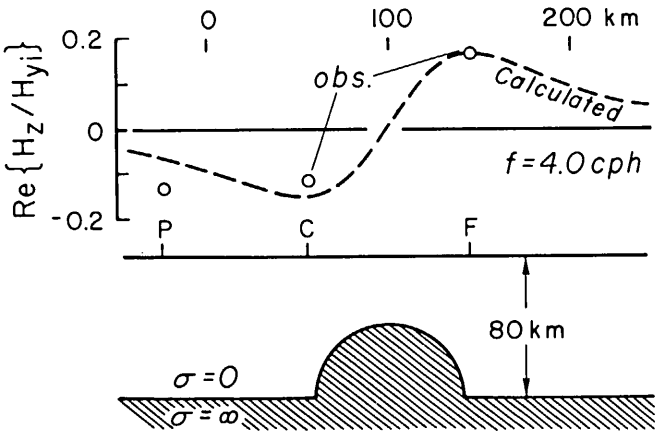

Figure 2. Observed and computed, normalized, in-phase, vertical magnetic field variation along WSW-ENE profile in western most Nevada. Also shown is simple, semi-cylindrical conductivity hump in the upper mantle which fits the observations. Urban centers located as abbreviations P (Pacific, CA), C (Carson City) and F (Fallon). Frequency is 4 cycles/hr. Adapted from Schmucker (1970).

Magnetotelluric Measurements

The magnetotelluric (MT) method, which makes use of both electric and magnetic natural field temporal variations, has been widely applied in the exploration of geothermal systems, sedimentary basins and the deep crust and upper mantle (Swift, 1967; Word et al., 1971; Vozoff, 1972; Larsen, 1975; Jupp and Vozoff, 1976; Stanley et al., 1977). While recent advances in instrumentation and data processing (Gamble et al., 1979; Weinstock and Overton, 1981; Stodt, 1983) enable accurate measurements of tensor MT responses, models of deep resistivity derived from MT responses commonly are suspect due to an unsatisfactory treatment of upper crustal lateral inhomogeneities (Wannamaker et al., 1983).

The Trouble with Upper Crustal Structure. - Serious problems with interpretation of MT soundings near electrically conductive graben sediments were first documented by Swift (1967) in his Arizona and New Mexico studies. A detailed

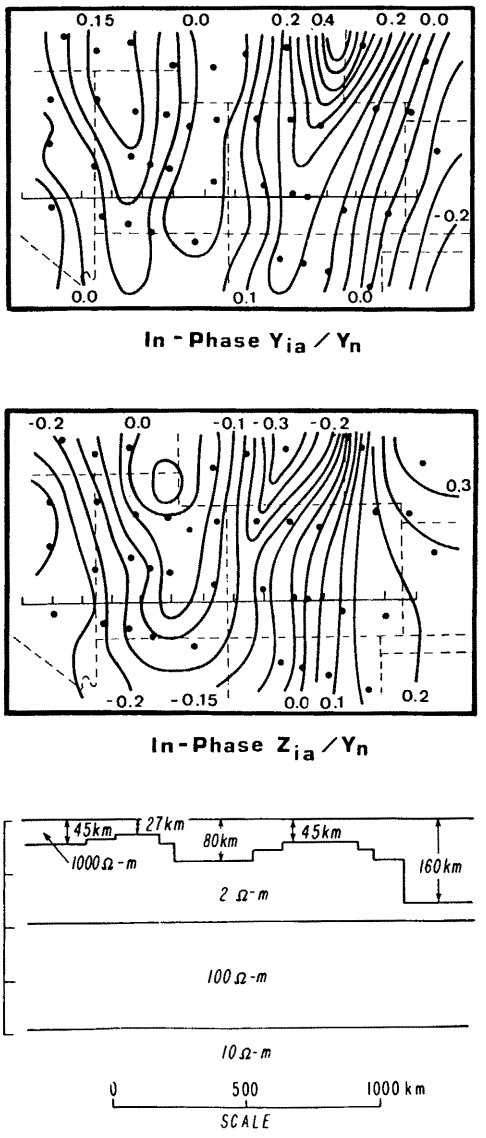

Figure 3. Normalized, anomalous, in-phase, horizontal E-W (Y_{ia}/Y_n) and vertical (Z_{ia}/Z_n) magnetic variation fields at a period of 60 minutes in the south western United States (Porath et al., 1970) along with the two-dimensional resistivity cross-section preferred by Porath (1971b) and Gough (1983) to explain the observations. The E-W profile for which the cross-section is defined is drawn on the maps of observed fields.

examination of the MT responses associated with graben alluvial fill has been performed by Wannamaker et al. (1983), who concluded that such responses are fundamentally three-dimensional in nature and that indiscriminate use of 1D or 2D modeling algorithms generally will incur serious errors.

Wannamaker et al. (1983) demonstrated in particular that two-dimensional transverse electric (TE) modeling algorithms are inappropriate for interpreting apparent resistivities, impedance phases or tipper in the northern Basin and Range identified as TE (Word et al., 1971; Vozoff, 1972). The 2D TE mode, consisting of the horizontal E-field parallel to strike and the orthogonal H-fields, involves no boundary charges and hence no current-gathering, whereas in the northern Basin and Range, all modes of MT responses due to upper crustal inhomogeneities are dominated by current-gathering.

If MT sounding data identified as TE in the presence of a 3D conductive inhomogeneity are inverted assuming a 1D model of deep resistivity structure, as I perceive has been overwhelmingly the case in the literature, then any such model will suffer systematically a compression of layer thicknesses and a downward bias in layer resistivities relative to the true 1D regional profile enclosing the inhomogeneity. This is because the TE mode apparent resistivity everywhere over and to the exterior of a conductive 3D body will be depressed throughout all frequencies relative to the apparent resistivity of the layered host containing the structure (Ting and Hohmann, 1981; Wannamaker et al., 1983).

Fortunately, accurate resistivity cross-sections through horst-graben morphology in the Great Basin can be obtained by selective application of a 2D transverse magnetic (TM) modeling algorithm (Wannamaker et al., 1983). The 2D TM mode consists of the H-field parallel to strike and the orthogonal E-fields. Boundary charges are included in both 3D and 2D TM formulations, allowing a proper treatment of current-gathering effects upon apparent resistivity and impedance phase. In defining data for transverse magnetic modeling of northern Basin and Range upper crustal structure, I recommend a uniform coordinate system based on tipper-strike (Vozoff, 1972). As with GDS transfer functions, tipper responses are band-limited in frequency (Wannamaker et al., 1983), so that one may choose an optimal frequency range for defining tipper-strike to minimize the contributions of secondary inhomogeneities much smaller than the conductive graben sediments for which one is primarily concerned in compensating.

MT Measurements at the Roosevelt Hot Springs.- A thorough accounting of upper crustal heterogeneity in the course of resolving deep resistivity has been performed on a collection of tensor MT data at the Roosevelt Hot Springs thermal area in S.W. Utah (Ward et al., 1978; Ross et al., 1982; see Figure 4). The complexly 3D nature of the MT responses directly over the thermal anomaly area prevented a rigorous quantification of any resistivity structure associated with an economic hot brine reservoir or a mid-crustal magmatic heat source for the geothermal system (ibid.). However, soundings along line B-B' in Figure 4 at distance from the thermal anomaly area, carefully modeled to remove the effects of upper crustal lateral inhomogeneities,

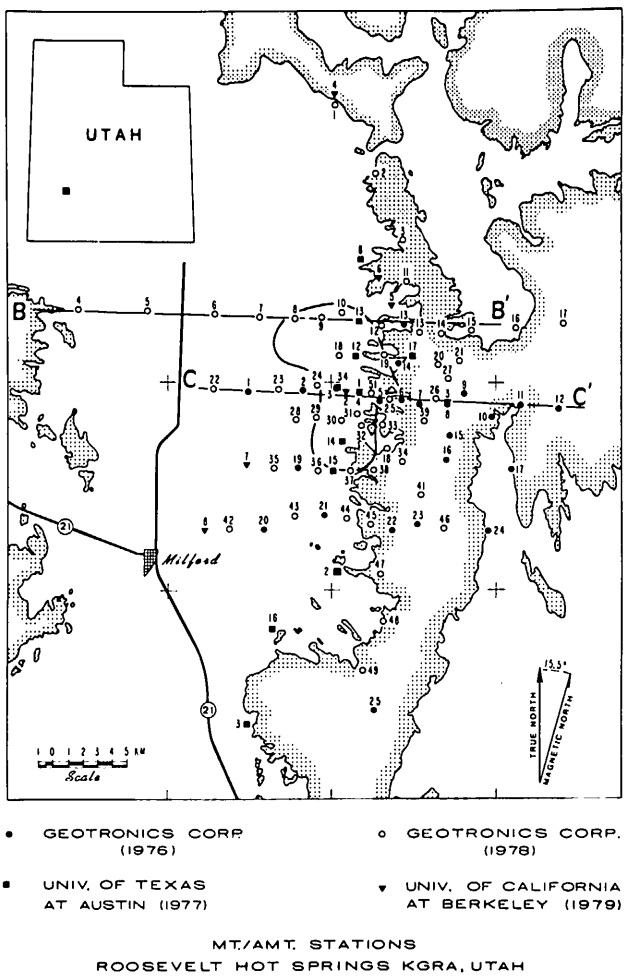

Figure 4. Magnetotelluric site location map for the Roosevelt Hot Springs thermal area. Rock outcrop bounding the Milford Valley sediments is lightly stippled while the solid curve is the 400 mWm^{-2} thermal contour (Ward et al., 1978). Station numbers referred to in text are prefixed according to the year in which they were occupied.

have yielded a regional resistivity profile for S.W. Utah to depths of about 100 km.

The observed quantities ρ_{yx} and ϕ_{yx} of line B-B', identified as TM, using a uniform coordinate direction as recommended previously, have been assembled in Figure 5 into pseudosections (Vozoff, 1972). The measured results for this line exhibit a virtually classic horst-graben response for the TM mode and bear a close resemblance to the computations of Wannamaker et al. (1983). Note especially the strong lateral gradients in ρ_{yx} and ϕ_{yx} between stations 78-8 and 78-10, which are due to the abrupt rangefront faulting bounding the graben sediments on the east side.

To interpret these MT observations, I have relied upon trial-and-error matching of results calculated from an assumed resistivity cross-section with the observed MT data of Figure 5 using a versatile and accurate 2D finite element forward program (Rijo, 1977; Stodt, 1978). Nonuniqueness in multidimensional modeling was alleviated by a high station density in each MT profile and by a wide spectrum of data at each station. In particular concerning the latter point, data at each sounding extended to sufficiently high frequencies so that both principal apparent resistivities ρ_{xy} and ρ_{yx}, as well as impedance phases ϕ_{xy} and ϕ_{yx}, have converged to common values above some frequency. For this high frequency range, the earth will likely be effectively one-dimensional, allowing one to constrain the near-surface model resistivities close to their true values. Such isotropic behavior occurs for frequencies above 1 Hz for the valley stations and above 30 Hz for the mountain sites.

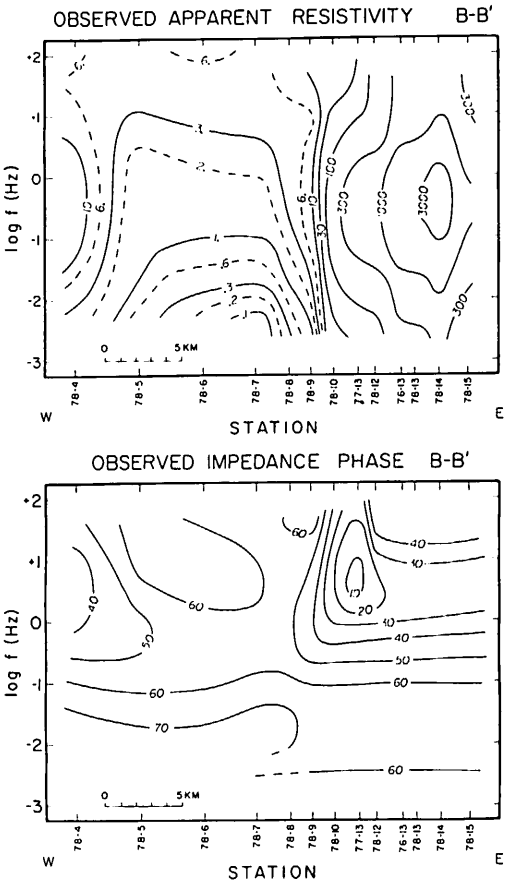

Figure 5. Observed pseudosections of ρ_{yx} and ϕ_{yx}, identified as transverse magnetic, along line B-B' of Figure 4. Contours of ρ_{yx} in Ω-m and of ϕ_{yx} in degrees.

The computed pseudosections of ρ_{yx} and ϕ_{yx} for line B-B' appear in Figure 6. Note that the computed and observed pseudosections are virtually identical; the observations have been fit to within data scatter almost everywhere. Examples of data scatter typical of sites over the Mineral Mountains will be forthcoming.

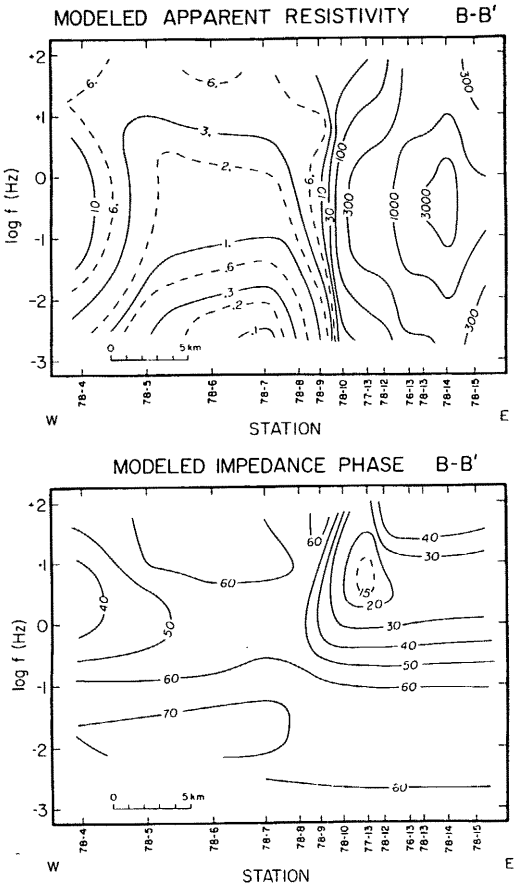

Figure 6. Best-fit pseudosections of ρ_{yx} and ϕ_{yx} obtained from transverse magnetic, finite element simulation of the observations of Figure 5. Contours of ρ_{yx} in Ω-m and of ϕ_{yx} in degrees.

The model of deep resistivity structure produced by application of the 2D TM finite element algorithm to the observations can be divided into two major parts: first, a shallow portion detailing just the extensive upper crustal lateral inhomogeneities in the upper 2 km; and second, a deep, purely layered portion extending to about 100 km which is determined by the physiochemical conditions of the crust and upper mantle below 2 km.

The upper 3 km of the finite element cross-section we have derived is shown in Figure 7. Within the Milford Valley, units within 140 m of the surface having resistivities from 3.5 to 18 Ω-m correspond to surficial clays, sands and gravels which are partially or completely water-saturated. Looking a bit deeper here, resistivities as low nearly as 1 Ω-m are caused by Pleistocene Lake Bonneville clays (Hintze, 1973, 1980), which we show residing to a maximum depth near 700 m below station 78-7. Deeper still exists a poorly resolved but substantial thickness (> 1 km) of modest resistivity material (25 Ω-m) related to pre-Bonneville alluvium and volcanics (Rowley et al., 1979). Note as well the especially steep dip of the eastern boundary faulting of the valley alluvium, inferred from the abrupt lateral gradients in ρ_{yx} and ϕ_{yx} between stations 78-9 and 78-10 in Figure 5 (cf. Wernicke and Burchfiel, 1982). The initial guess in the modeling process of this upper crustal resistivity section was guided by the refraction seismic model of Gertson and Smith (1979) and the gravity observations of Carter and Cook (1978), but the final section in Figure 7 shows important differences.

Over the Mineral Mountains, our model in Figure 7 shows resistivities of hundreds of ohm-m increasing to 3000 Ω-m over the depth interval of 2 to 3 km. This represents a decrease in porosity of the well-indurated basement rocks to well under 1%, probably due for the greater part to a decrease in fracture porosity below 2 to 3 km depth.

The 1400 Ω-m medium in Figure 7 begins the deep layered resistivity profile introduced previously and shown in its entirety in Figure 8. The best-fit model shows a maximum resistivity of 3000 Ω-m over the depth interval of 3 to 11 km. Subsequently, resistivity falls to 200 Ω-m by 35 km depth, whereupon an abrupt drop to 20 Ω-m is encountered. This low-resistivity material defines a deep, thick layer bottomed at 65 km depth by a sudden increase to a 200 Ω-m basal half-space. The fact that this deeper part of the model is purely layered is not due to poor resolution on the part of the measurements of Figure 5; the data quality for all soundings in line B-B' is good to excellent and yet the data are fit within scatter by imposing a purely 1D section for depths greater than 2 km. Furthermore, through application of a 2D TM program, the data of line C-C' in Figure 4 also are fit using the preferred deep profile of Figure 8 (Ross et al., 1982).

In Figure 9 are plotted both modes of apparent resistivity and impedance phase for station 76-13 along with several computed response curves. First, consider the solid curves passing through the observed data points of ρ_{yx} and ϕ_{yx}. These curves display the calculated response of the best-fit finite element model of Figures 7 and 8 at station 76-13, a response which seems very agreeable with the trends of the observed data points. In addition, curves of long dashes lying intermediate to the principal apparent resistivity and impedance phase observations are shown in Figure 9. The response of the best-fit one-dimensional deep resistivity profile of Figure 8 in the absence of all upper crustal lateral

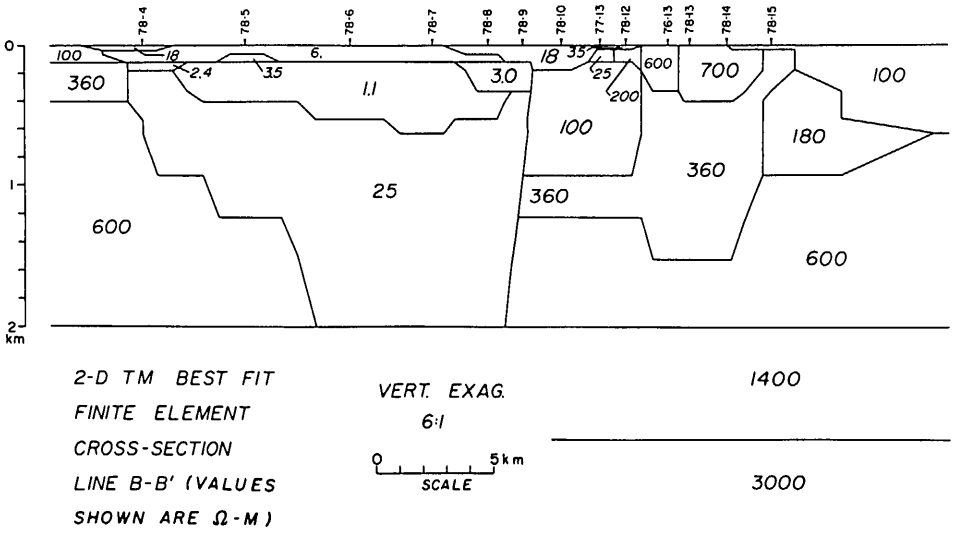

Figure 7. Best-fit, 2D TM finite element resistivity cross-section fitting the observations of line B-B' in Figure 4.

structure is represented by these latter curves. The difference between the observations and the purely 1D response illustrates again the importance of the Milford Valley in determining the MT signatures in this area. The inclusion of lateral inhomogeneities in models of deep resistivity structure is of paramount importance in tectonically disturbed regions like the Great Basin, and supercedes other considerations of the appropriateness of resistivity models vis-a-vis continuous vs. layered one-dimensional structures (Larsen, 1981; Parker and Whaler, 1981).

I turn now to resolution of detail in the deep resistivity profile of Figure 9. It is noted at the outset that, while lateral inhomogeneities, i.e., the Milford Valley, have induced anisotropy to a high degree over the Mineral Mountains, both tensor and 1D signatures in Figure 9 bear a certain mutual resemblance. In particular, the factor of ten drop in model resistivity at 35 km depth is responsible for the particularly steep gradients in the apparent resistivities and the values of impedance phases about 70° around 0.03 Hz. Also, without the abrupt rise in model resistivity at 65 km depth, the apparent resistivity data would not flatten out nor would the impedance phase data fall as strongly or rapidly as they do in Figure 9 at the lowest frequencies, especially below 0.003 Hz.

At frequencies less than 0.01 Hz in Figure 9, both ϕ_{xy} and ϕ_{yx} have converged to common values while ρ_{xy} and ρ_{yx} have shapes that are essentially identical except that they are offset by a factor of ten. Eventually, a convergence of this sort occurs as frequency falls for all stations in the Roosevelt Hot Springs area. This frequency dependence of the tensor sounding curves particularly illustrates that a one-dimensional, regional resistivity profile containing local lateral variations in structure, chiefly the Milford Valley sediments, is a viable model for the resistivity makeup here in S.W. Utah.

To strengthen confidence in the best-fit deep resistivity profile, I consider three alternates in Figure 8. The first is a profile whose log resistivity decreases linearly with depth (plotted with dots and labelled the "Steady Decrease" model in Figure 8). I arrive at a second layered sequence drawn with alternating dots and dashes in Figure 8 and called the "Shallow" regional model by shrinking the depths and resistivities of individual layers by 30% such that layer contrasts and conductivity thickness products remain constant (Madden, 1971). The last parameter resolution examination deals solely with the deep low-resistivity layer from 35 to 65 km. I maintain that this 20 Ω-m medium is not a "thin" layer (Madden, 1971), and to prove so it is replaced by a unit of equivalent conductivity-thickness product of 10 Ω-m resistivity and 15 km thickness.

The TM mode computed response curves at site 76-13 for the valley cross-section contained in each of the alternate model regional profiles appear in Figure 9. The computed apparent resistivity or impedance phase or both for each of the alternate models do not fit the observed data points over much of the frequency range, causing them to be dismissed as candidates for deep resistivity structure in this area. Recall that all soundings on profiles B-B' and C-C' are explained using the same regional profile; several other soundings in the Mineral Mountains are comparable in quality to site 76-13 and show

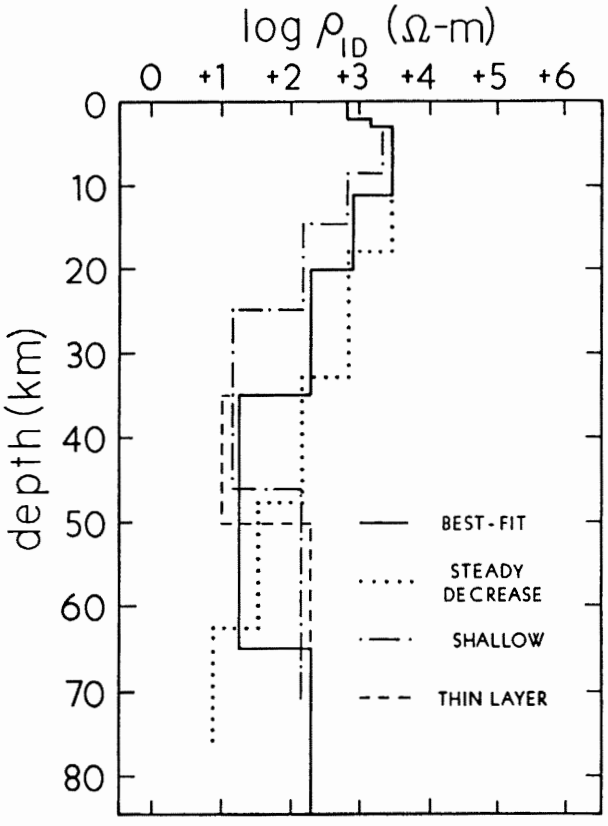

Figure 8. One-dimensional, deep resistivity profile in this area of S.W. Utah defining the lower portion of our 2D finite element model. Alternate resistivity profiles used in parameter resolution tests are drawn with dots and dashes.

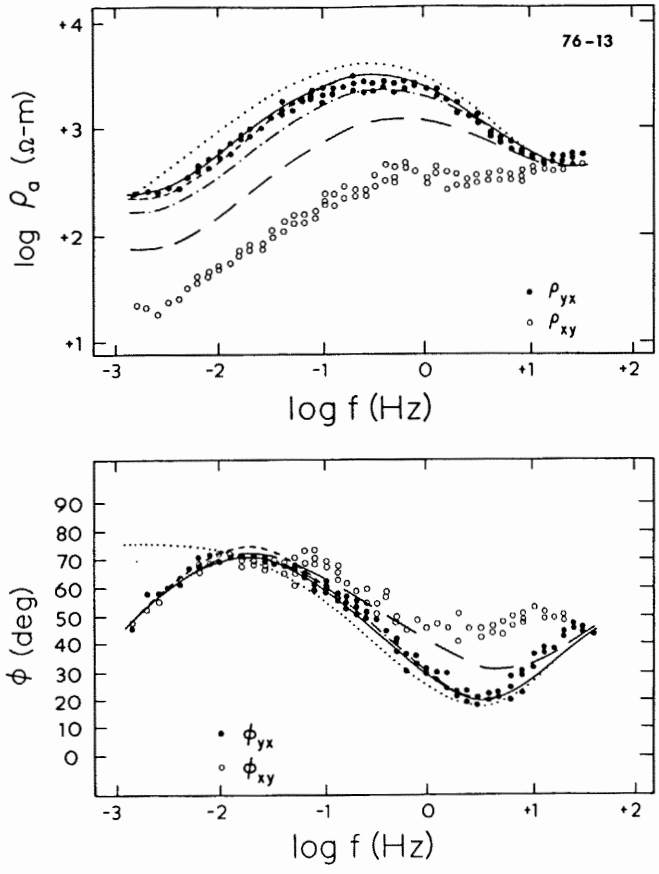

Figure 9. Observed data ρ_{xy}, ρ_{yx}, ϕ_{xy} and ϕ_{yx} for sounding 76-13 of line B-B'. Solid curve represents goodness-of-fit of computed to observed results using the best-fit resistivity cross-sections of Figures 7 and 8. Curves of dots and shorter dashes relate to correspondingly drawn alternate resistivity profiles in Figure 8 used in parameter resolution tests. Curves of long dashes appearing between the two modes of data points represent the 1D forward computation using the best-fit regional profile in Figure 8.

equally well the inadequacy of the alternate regional profiles. I presume a maximum depth of sensitivity of the data to subsurface structure of about 120 km, as imposition of low-resistivity material here causes computed phases at 0.002 Hz which exeed those of the best-fit model by about four degrees and which cannot be made to agree with the observations by increasing the resistivity of the 200 Ω-m material.

Before closing this particular study, there is one more demonstration of the hazards of 1D interpretation of MT data in regions of extension like the northern Basin and Range. In Figure 10 are reproduced the best-fit deep profile of Figure 8 as well as model profiles computed through direct 1D inversion of the tensor MT observations of Figure 9 (I used the routine of Petrick et al., 1977). The display of these observations with the computed 1D responses of the aforesaid model profiles in Figure 11 shows the goodness of fit possible by a 1D inversion algorithm to data taken in 3D environments. The deep resistivity models derived thereby are unacceptable, however; their departure from the preferred deep profile exceeds bounds that were already rejected in the rigorous parameter resolution studies of Figures 8 and 9. Moreover, due to local lateral inhomogeneity, computed layered models will vary drastically from site to site within the mountains, underscoring the unreliability of one-dimensional inversion in this environment.

Matters are even worse for 1D inversion of MT soundings taken within northern Basin and Range graben fill. Figure 12 shows layered earths computed through 1D inversion of apparent resistivities ρ_{xy} and ρ_{yx} and impedance phases ϕ_{xy} and ϕ_{yx}, identified as TE and TM (Word et al., 1971; Vozoff, 1972), for site 78-6 of Figure 4. Solid curves through the data in Figure 13 show

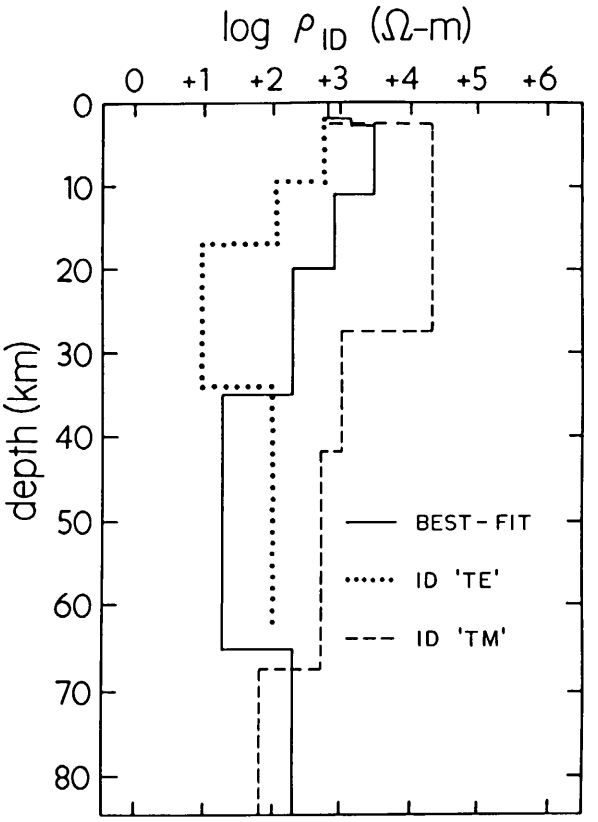

Figure 10. Best-fit regional resistivity profile for the Roosevelt Hot Springs thermal area compared to layered models obtained through 1D inversion of ρ_{xy} and ϕ_{xy} (dotted lines) and ρ_{yx} and ϕ_{yx} (dashed lines).

the goodness-of-fit obtained by the inversion, with the nominally very conductive basal half-spaces resolved by the observations below 0.2 Hz. However, given the best-fit model of Figure 8 derived through a rigorous accounting for the effects of the valley sediments, the layered models at site 78-6 are obviously unrealistic. Note that the data of Figure 13 bear a close resemblance to the theoretical computations of Wannamaker et al. (1983) over their model valley. I believe that 1D models of resistivity given by Stanley et al. (1976) for the Stillwater-Soda Lakes district, which were computed from soundings taken within deep conductive alluvium of the Carson Sink area, are similarly affected. The case for low resistivities at depths as little as 5 km in that region remains to be substantiated.

Physical State at Depth in S.W. Utah. - In Figure 14, the best-fit regional profile for the Roosevelt Hot Springs is compared to laboratory experiments on the electrical properties of rocks. A crustal thickness slightly less than 30 km is assumed for this area (Keller et al., 1979; Allmendinger et al., 1983). Petrological studies and seismic velocities point to a mafic

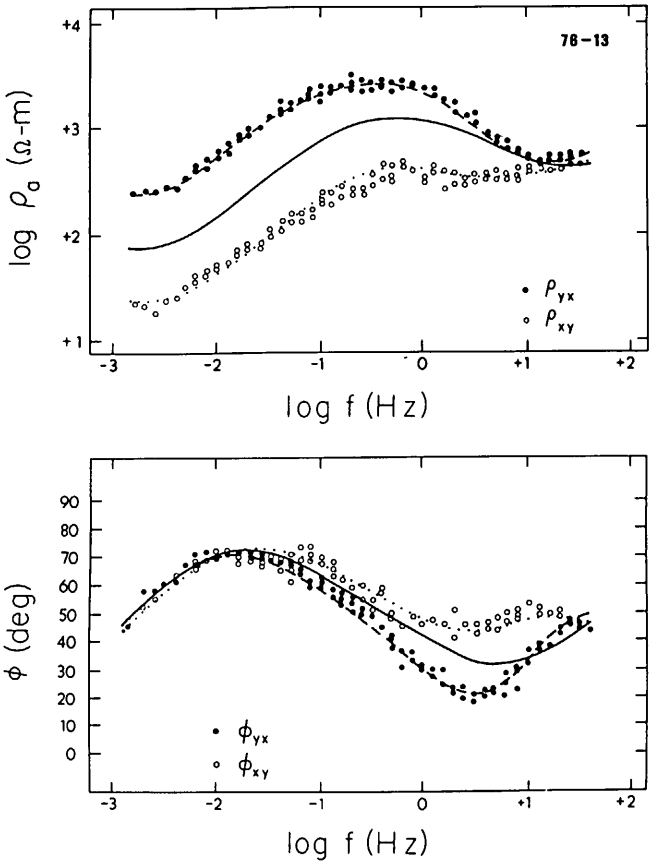

Figure 11. Observed data points of ρ_{xy}, ρ_{yx}, ϕ_{xy} and ϕ_{yx} for sounding 76-13 showing the goodness of fit that can be obtained to 3D data using a 1D inverse routine. However, the resultant layered models were dismissed as unrealistic. Solid curve appearing between data points is the 1D forward response of the best-fit regional profile.

metaigneous composition near gabbro for most of the lower half of the crustal section, with relatively felsic rocks above (Smith, 1978; Padovani et al., 1982; Nash, 1983). A peridotite composition is taken for the upper mantle rocks (Wyllie, 1979).

Adopting a conductive geotherm for a regional heat flow of 2.4 HFU (1 HFU = 41.6 mWm^{-2}) (Lachenbruch and Sass, 1978; Chapman et al., 1981), the lower bound on aqueous electrolytic conduction through rock pores of Brace (1971) and the mean dry gabbro semiconductivity results of Kariya and Shankland (1983) are combined to yield the curve of dots in Figure 14. Over the depth interval 15 to 30 km, the regional profile appears somewhat less resistive than what is predicted by dry solid-state measurements. If a gabbroic

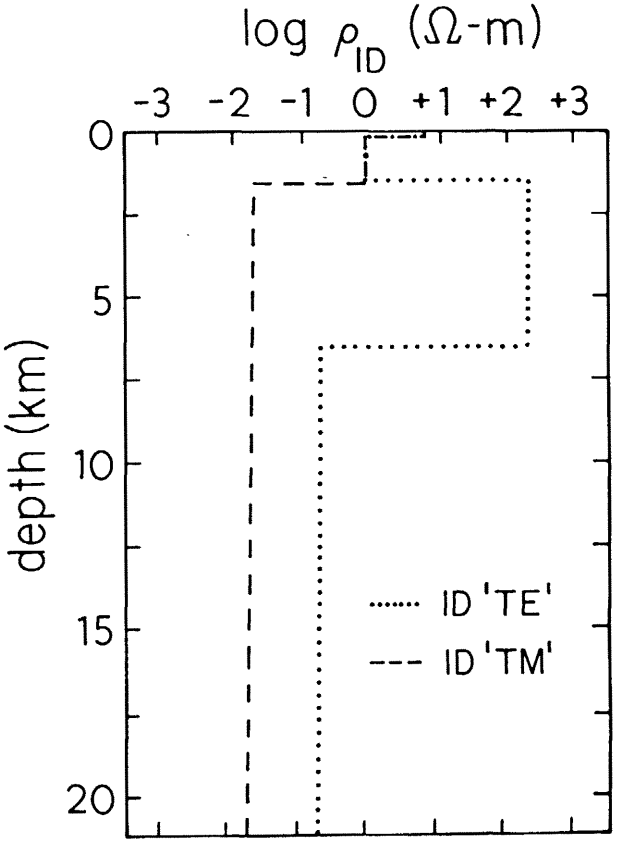

Figure 12. Layered resistivity models obtained through 1D inversion of ρ_{xy} and ϕ_{xy} (dotted lines) and ρ_{yx} and ϕ_{yx} (dashed lines) for sounding 78-6 of Figure 4. Note scale change from Figure 10.

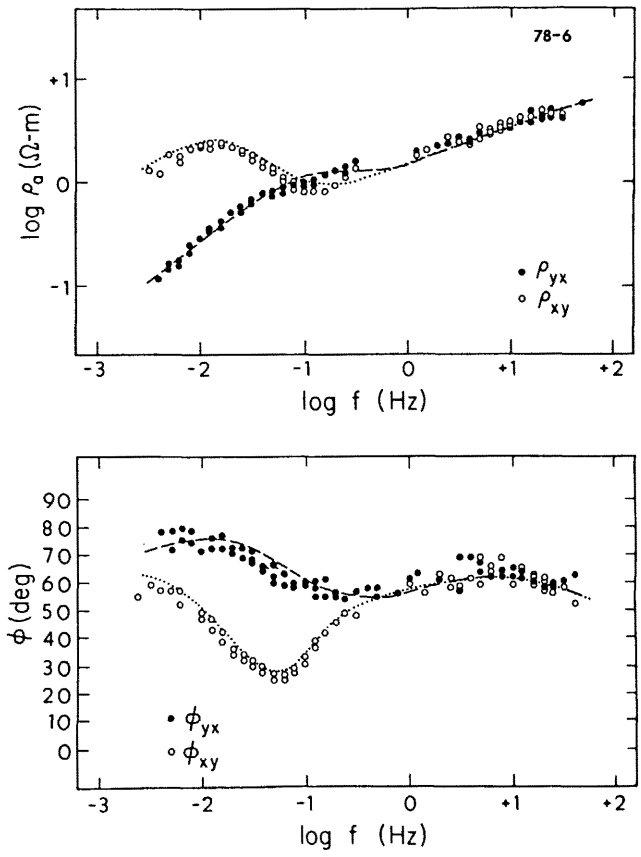

Figure 13. Observed data points of ρ_{xy}, ρ_{yx}, ϕ_{xy} and ϕ_{yx} for sounding 78-6. Curves of dots and dashes show responses of layered earth models of Figure 12.

composition is relevant then free water in this interval is improbable (Burnham, 1979a, 1979b). However, a reduction of solid-state resistivity through active deformation and non-zero partial pressure of water appears possible (Winkler, 1979; Duba and Heard, 1980; Kirby, 1983; Spear and Silverstone, 1983).

The curve of dashes in Figure 14 pertains to upper mantle rocks and results from the solid-state measurements on olivine by Duba et al. (1974) and the conductive geotherm. Of greatest importance, the shape of the solid-state curve is very different from the regional profile. In an earth where temperature increases steadily with depth, such as is the case with our conductive geotherm or even with any of the temperature profiles of Lachenbruch and Sass (1978) which incorporate convective components, the Arrhenius solid-state temperature dependence for a rock results in bulk resistivity which decreases monotonically with depth. During the discussion of parameter resolution, a deep resistivity profile that decreased steadily with depth was rejected as a candidate to explain the low-frequency MT observations in S.W. Utah; the order-of-magnitude rise of resistivity in the upper mantle in our best-fit deep model is a strict requirement.

I therefore look to partial melting in the upper mantle as the cause of the 20 Ω-m deep layer. Again imposing the conductive geotherm, the curve of dots and dashes in Figure 14 arises using a dry peridotite melting curve (Mysen and Kushiro, 1977; Wyllie, 1979; Best et al., 1980), the measurements of alkali-olivine basalt conductivity of Rai and Manghnani (1978) and the melt phase interconnection model of Waff and Bulau (1979). The large liquid fractions implied by this melting curve are of course unrealistic and result from use of a conductive temperature profile. Given that melt conductivities are strongly temperature dependent, and that the interconnection model is strictly an abstraction, I simply conclude that the melt fraction in the deep, low-resistivity layer is rather small, less than 5%. In reality, the dry peridotite solidus is advocated as a representative pressure-temperature trajectory for the depth interval of the 20 Ω-m layer (Mysen and Kushiro, 1977; Wyllie, 1979; Best et al., 1980). It is argued shortly that this trajectory may be valid to much greater depths in the region.

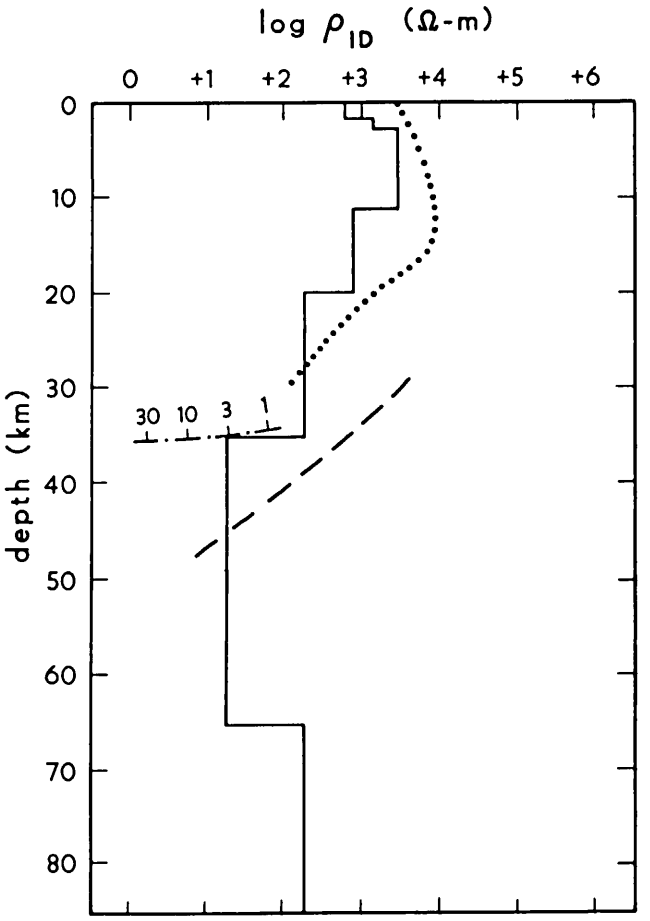

Figure 14. Best-fit, crust and upper mantle resistivity profile for southwestern Utah compared to physical model incorporating aqueous electrolytic conduction in rock pores, solid-state semiconduction in minerals and ionic conduction in partial melts. Definition of curves explained in text.

Controlled-Source EM Techniques

In controlled-source electromagnetics (CSEM), EM fields are impressed by a transmitter, either fixed-site or roving, and monitored as a function of position and/or frequency at a receiver (Grant and West, 1965; Ward, 1967). The current transmitter can be a grounded bipole, an ungrounded loop, or a very long, essentially ungrounded line source.

Effects of Upper Crustal Structure. - Ward (1983) has investigated theoretically the behavior of EM fields about typical northern Basin and Range alluvial fill for grounded bipoles and an ungrounded loop. The basin model he has chosen has a resistivity and dimensions similar to that of Wannamaker et al. (1983), except that Ward's model was enclosed simply in a 400 Ω-m half-space. The frequency of excitation was 0.03 Hz.

The difference between the total field in the presence of the valley and the half-space host field is a measure of the error in models of deep resistivity profiles derived from simple 1D inversion. For the grounded bipole source of Ward (1983) the amplitude of the horizontal magnetic field over the body rose to more than 3 times the primary field. It asymptotes to 60% of the primary field at large distances from the body. Channeling of the bipole return current through the valley fill can explain this result. Distortions of the horizontal H-field were as severe for the square loop as for the grounded bipole. The importance of this latter behavior cannot be overemphasized; total and primary fields differ to extremely large distances and to low frequencies even for ungrounded sources.

Models of Deep Resistivity from CSEM. - Experiments using galvanic resistivity methods in the northern Basin and Range and the Colorado Plateau by the U.S. Geological Survey have been summarized by Keller (1971). As Keller stated, the techniques used at the time were largely experimental and developmental, and were sensitive only to conductive graben sediments overlying a resistive rock basement.

In 1977, multifrequency dipole-dipole (3 and 6 km dipoles, separations to n = 6) galvanic resistivity measurements were made in southwestern Utah by the Department of Geology and Geophysics, University of Utah, in an attempt to describe any resistivity structure associated with the Pioche-Marysvale trend (Rowley et al., 1979; Petrick et al., 1981). The data, from a profile extending 33 km northward from the Roosevelt Hot Springs, were dominated to an unexpectedly severe degree by upper crustal, 3D lateral inhomogeneities, especially graben sedimentary fill. These inhomogeneities lead to a lack of fit of layered inverse calculations to observed data, as well as dubious 1D and 2D earth models (W.R. Petrick and A.C. Tripp, unpub.). A 3D inversion of these results (Petrick et al., 1981) presents a concentration of low-resistivity structure within 2 km of the surface, evidence again of variable basin fill dominating the observations.

Towle (1980), utilizing an interstate power transmission line as a long grounded bipole, has studied deep resistivity in eastern California with direct current magnetic field variations. A waiting period of 10 minutes was necessary to allow transients in the current to decay to negligible levels. Towle's data is consistent with a shallow return current concentration lying east of the Sierran Front in fractured rocks and sediments in the uppermost crust of the Basin and Range.

Assuming the same interstate power system as Towle to be an essentially ungrounded AC line source of current, Lienert and Bennett (1977) and Lienert (1979) advanced 1D models of resistivity

in eastern California and western Nevada to depths of 40 to 50 km. Included in their interpretation was 10-15 km thick layer of low resistivity (10-30 Ω-m) whose depth to top varied from 20 to 30 km (Figure 15). However, in light of Towle's experience, it appears that grounding terms were very important over the frequency range employed in the survey areas of Lienert and Bennett (1977) and Lienert (1979) (6-42 cycles/hr). Moreover, these authors did not evaluate quantitatively the effects of the 3D sedimentary basins common in their areas. It was shown by Ward (1983) that these structures can cause widespread distortions of EM fields to low frequencies even for ungrounded sources. Given these points, I do not believe their results demonstrated with certainty that a resistivity minimum exists in the lower crust.

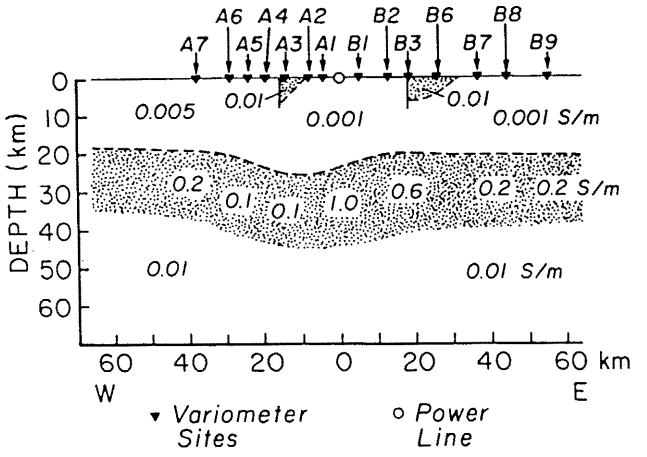

Figure 15. Cross-section of model conductivity structure beneath the Walker Lake, Nevada, district. Profile location also shown on Figure 1. Modified from Lienert and Bennett (1977).

Wilt et al. (1982) have described low-frequency CSEM soundings in the Buena Vista valley of N.W. Nevada. Through 1D inversion of the data, these authors advocate low resistivity (2-7 Ω-m) at depths of 4-7 km in basement rocks beneath the valley. A 1D inversion of a nearby MT sounding in the valley also showed relatively low resistivities ($\sim$ 25 Ω-m) at rather shallow depths ($\sim$ 11 km). However, Wilt et al. admit that preliminary 2D modeling suggests that 1D inversion of their CSEM data in the presence of the valley underestimated depth to conductive basement. Given the 3D model simulations of valley fill by Ward (1983) and Wannamaker et al. (1983) and the experience at the Roosevelt Hot Springs discussed previously, I take the approximate agreement between the 1D MT and 1D CSEM models at Buena Vista valley as further evidence that graben sediments seriously disrupt the CSEM observations. Again, I believe the case for widespread low resistivities at shallow depths in basement rocks of the Great Basin remains quite uncertain.

TECTONIC SIGNIFICANCE OF NORTHERN BASIN AND RANGE RESISTIVITY

The interpretation of deep resistivity at the Roosevelt Hot Springs has provided a point sampling of physiochemical conditions at depth in S.W. Utah. However, comprehension of these conditions will require consideration of the tectonic evolution of the northeastern Basin and Range during Late Cenozoic time. The model of resistivity and its implications finally are extended to the northern Basin and Range as a whole.

Evolution of Resistivity in the Northeastern Basin and Range

It is noted at the outset that the depth interval of interconnected basaltic melt corresponding to the 20 Ω-m layer in Figure 14 is significantly shallower than the seismic low-velocity zones of either the northern Basin and Range interior or the Colorado Plateau (Priestley and Brune, 1978; Thompson and Zoback, 1979), which are also interpreted to reflect partial melting in the upper mantle (Wyllie, 1979). These apparently disparate geological environments can be reconciled, with help from geomagnetic deep sounding anomalies and concepts of regional tectonic setting.

Diapirism and Melting. - Of paramount importance in fitting the deep physical state inferred in S.W. Utah to those of neighbouring regions is the well-documented, progressive concentration of extensional tectonism throughout the northeastern Basin and Range during the last 8-9 m.y. (e.g. Christiansen and McKee, 1978; Smith, 1978; Stewart, 1978; Rowley et al., 1979; Thompson and Zoback, 1979). This concentration has resulted in crustal thinning, low upper mantle velocities, bimodal volcanism and heat flow which are anomalous compared to the northern Basin and Range interior of central Nevada (Figures 16-19).

While much lithospheric extension throughout the northern Basin and Range prior to Mid-Miocene time may have been due to intrusion of calc-alkaline magmas derived ultimately from melting in the upper mantle associated with Farallon plate subduction (Zoback et al., 1981), such intrusion alone probably does not thin the crust (Gastil, 1979; Eaton, 1982). The Late Miocene to present extension defining today's horst graben morphology, however, is broadly distributed and indicates stretching and upwelling of both the crust and the upper mantle. Crustal thicknesses determined seismically hence can be used as a guide to average extension rates since the Late Miocene (see Figure 16).

If a value of 44 km for the thickness of the Colorado Plateau crust (Keller et al., 1979) can be used as a guide, then crustal thicknesses imply an average rate of extension of nearly 2% per m.y. for the northern Basin and Range interior of east-central Nevada in the last 10-12 m.y. However,

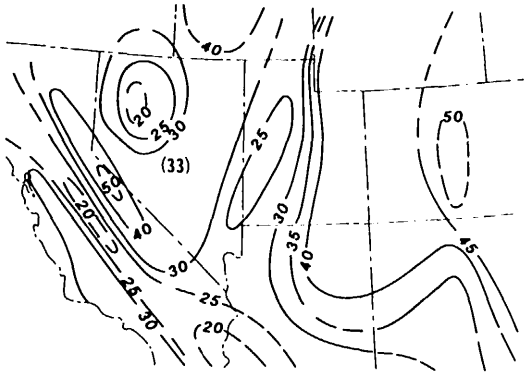

Figure 16. Crustal thicknesses in the south western United States. Contour values in kilometers. From Smith (1978), Keller et al. (1979) and Priestly et al. (1980).

about 5% per m.y. is implied for much of the northeastern Basin and Range during the last 8-9 m.y. If so, then a 1D estimate of upward velocity v of material at depth (related linearly to extension rate s and depth z through v = sz; Lachenbruch and Sass, 1978) ranges from about 1 1/2 km/m.y. at 35 km through 5 km/m.y. at 100 km to over 7 km/m.y. at 160 km.

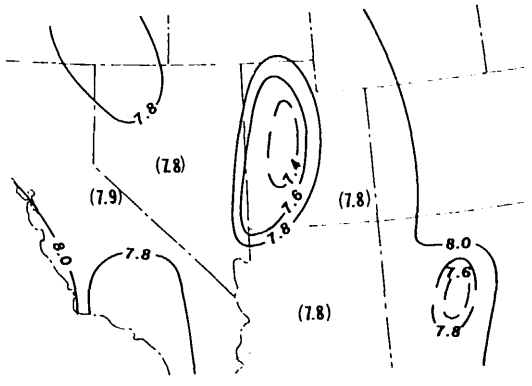

Figure 17. Uppermost mantle compressional (P_n) velocities. Contour values in km/s. From Smith (1978) and Keller et al. (1979).

While contributing a great deal to surface heat flow and temperatures within the lithosphere (Lachenbruch and Sass, 1978), extension rates tell something about the thermal state at greater depths as well. Consider for simplicity a spherical diapir in the upper mantle of radius 50 km, a representative E-W length scale for the region of enhanced tectonism defining the northeastern Basin and Range. For the thermal state of a rising diapir to be largely adiabatic (Oxburgh, 1980), its ascent time must be less than its thermal conduction time constant (Spera, 1980). If the hypothetical spherical diapir has been rising with a velocity v = 5 km/m.y. from a depth of 100 km or so during the last 8 m.y., then a distance of roughly 40 km would have been covered. In covering this distance, the diapir ascent rate merely must exceed about 0.40 km/m.y. (Spera, 1980), much less than v, for the aforesaid thermal inequality to be met. One may conclude that large volumes rising here in the upper mantle tend to retain much of their sensible heat during transport.

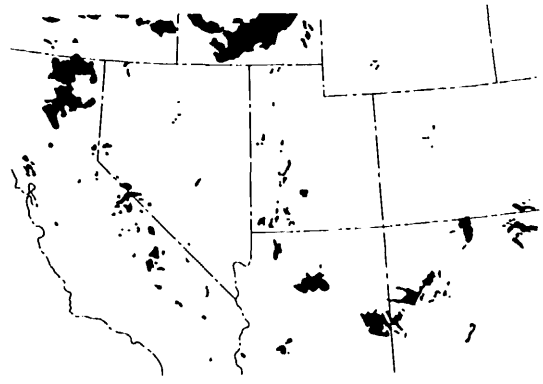

Figure 18. Distribution of volcanics less than 5 m.y. old. From Christiansen and McKee (1978), Ward et al. (1978) and Luedke and Smith (1978a, 1978b, 1981).

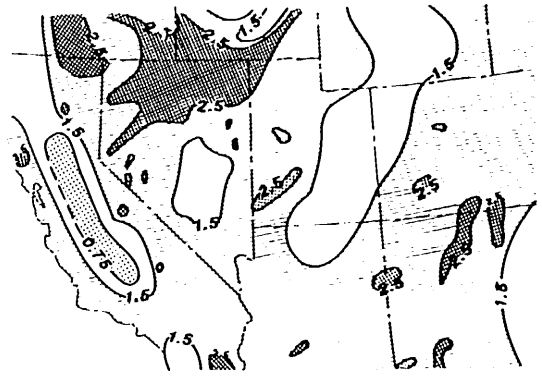

Figure 19. Surface heat flow contours in heat flow units. From Sass et al. (1981) and Bodell and Chapman (1982).

As a mass at depth rises adiabatically, its temperature trajectory may intersect the peridotite solidus so that melting will proceed (Yoder, 1976). Upon crossing the solidus, the temperature within the ascending diapir is buffered by the melting behavior of peridotite (Oxburgh, 1980). In particular, the great size of the latent heat of fusion relative to the heat capacity of peridotite along with the nearly invariant nature of basalt production serve to keep the temperature gradient within the diapir well within 1 °C/km of the solidus during adiabatic ascent (Yoder, 1976; Mysen and Kushiro,

1977; Oxburgh, 1980; Turcotte, 1982). The degree of melting is inevitably subdued through heat loss to the earth's surface from the top of the diapir (Spera, 1980).

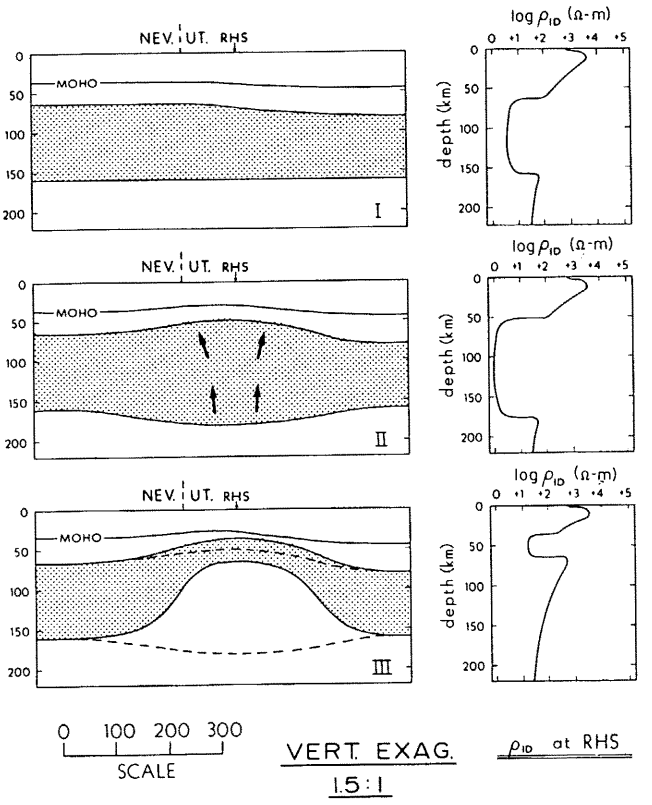

Figure 20. Schematic, highly simplified, three-stage model of evolution of resistivity structure in the eastern Great Basin. The region of continuous interconnection of melt in the upper mantle is defined by stippling and the predicted deep resistivity profile beneath the eastern Great Basin at each stage is drawn at the right side of diagram.

With this brief discussion of diapirism, I advance a schematic and highly simplified model for the Late Cenozoic evolution of deep resistivity in the northeastern Basin and Range. The model is depicted in Figure 20 in three stages: I, by about 10 m.y. ago, extensional activity responsible for the present horst-graben morphology had spread throughout the northern Basin and Range. Attendant upwelling of mantle peridotite had resulted in widely distributed, fundamentally basaltic volcanism, presumably involving the mechanism of decompression just described, along with a layer of partial melt of low melt fraction ($\sim$ 5%) which did not differ greatly from that defining the present seismic low-velocity zone of central Nevada; II, by 8 m.y. ago, the well-documented concentration of extension in the northeastern Basin and Range was underway. Accelerated diapiric uprise of mantle material leads to a further amplification of the thickness and degree of melting of the LVZ. The extent of the amplification is difficult to gauge, as it depends on the degree to which the geotherm just above and just below the former LVZ was superadiabatic (Oxburgh, 1980); III, the melt fraction in the magnified zone of fusion can build up only to a point, after which much of it drains buoyantly upward. This convection of basalts, which in effect are superheated with respect to the environment into which they rise, advances the front of melting to 35 km depth and helps establish the realm of interconnected melt corresponding to the 20 Ω-m layer of Figure 14 by warming the host peridotite during passage.

The model of present distribution of partial melting in the upper mantle of the northern Basin and Range and western Colorado Plateau in Figure 20 is similar to that of Thompson and Zoback (1979). The latter authors utilize the resistivity model of Porath (1971), however, to suggest that interconnected melt exists to a depth of about 160 km beneath the northeastern Basin and Range. Nevertheless, the magnetotelluric data preclude such an interconnection below about 65 km and the resolution by geomagnetic deep sounding of such details is doubtful (Gough, 1983). Given the chemistry of certain basaltic lavas in the northeastern Basin and Range (Wyllie, 1979; Best et al., 1980) and our model of diapiric upwelling, some melting events are probable at depths well below 65 km - they just don't result in a broad zone of interconnected liquid. On the other hand, the uniqueness of the model of Thompson and Zoback beneath the northeastern Basin and Range must be questioned.

I suggest that the zone of interconnected melt below S.W. Utah lies where it is because the very much reduced rigidity of the crystalline peridotite matrix at greater depths (Darot and Gueguen, 1981) promotes both the formation of vertical fissures under tensile stress (Spera, 1980) and the ductile collapse of the crystalline matrix as the melt leaves to enter the fissures (Stolper et al., 1981; Turcotte, 1982). In addition, any melt percolating up from great depth along intergranular passageways (Turcotte, 1982) would be impeded from rising beyond the zone of our low resistivity layer by the increasingly stiff rheology of peridotite.

Thermal State at Depth in the Eastern Great Basin. - Previously, I assigned a temperature trajectory through the deep low-resistivity layer that was coincident with the dry peridotite solidus (nominally that of Wyllie, 1979). Based upon compositions of basalts in S.W. Utah, such a thermal profile seems appropriate to depths near 100 km (op. cit.). In fact, if the abstraction of adiabatic diapiric uprise in the northeastern Basin and Range is favored, a dry solidus trajectory may be definitive to a depth exceeding 160 km.

In Figure 14, a conductive geotherm based

upon a regional heat flow of 2.4 HFU for S.W. Utah predicted fusion of dry peridotite at essentially the same depth as the top of the model low-resistivity layer. However, with the high extension rates proposed for the northeastern Basin and Range, the foregoing coincidence should not be (Lachenbruch and Sass, 1978). As a simple example, purely solid-state stretching at a rate of 5% per m.y. is consistent with a depth of melting of nearly 40 km, but a surface heat flux reaching 3 HFU is to be expected (ibid.).

One would conclude on this basis that the crust and upper mantle of northeastern Basin and Range has not reached a steady thermal state. The onset of extension is fundamentally an increase of heat flux into the lithosphere, and adjustment of surface heat flow to this form of thermal disturbance may take longer than the 8 m.y. inferred as the interval of concentrated extension in the northeastern Basin and Range (Lachenbruch and Sass, 1978; Rowley et al., 1979). By coincidence, a conductive geotherm based on present surface heat flow and a non-equilibrium convective geotherm considering the concentration of extension in the northeastern Basin and Range do not differ greatly.

Application of Interpretation to Other Areas

Attenuated crustal thicknesses in northwestern Nevada (Figure 16a), the pronounced extension near Yerrington interpreted by Proffett (1977) and the concentration of rifting, heat flow and volcanism in western Nevada and southeastern California (Figure 16b-d) indicate that the western margin of the northern Basin and Range experiences an enhanced degree of extension relative to the northern Basin and Range interior. The similarity in tectonic styles between the eastern and western margins of the northern Basin and Range suggests that a deep electrical structure corresponding to Stage III of Figure 17 is likeliest for the northwestern Basin and Range. The deep resistivity investigation by Schmucker (1970) permits this conclusion, but does not uniquely favor it given the limited resolution.

Another tectonic environment which probably fits into the framework of Figure 17 is the Rio Grande Rift and nearby regions. Of particular interest is the continuation of this rift zone northward into Colorado. As described by Williams (1982), extensional deformation and volcanism diminishes in this direction although some Late Tertiary mafic volcanism persists into Wyoming. In light of the modest degree of extension, I propose that the continuation of the Rio Grande Rift into Colorado may be a good place to search for deep electrical structure representing Stage II in Figure 17. The northward increase in geomagnetic deep sounding anomalies in this area (Figure 3) is furthermore suggestive of this notion, but magnetotelluric profiling with a proper multidimensional interpretation is needed to assess accurately the deep resistivity section here.

CONCLUSIONS

In active extensional environments, significant temperature perturbations may exist, possibly with interconnected melt phases, creating lateral and vertical contrasts in resistivity of an order-of-magnitude or greater. Unluckily, such environments also are attended to a large degree by upper crustal lateral inhomogeneities, especially graben sedimentary fill, whose resistivity contrast with the surrounding rock host is at least as high as that of the structures of interest at depth, and whose proximity to the surface obscures the interpretation of deep targets using electromagnetic measurements.

However, there is generally a strong preferred orientation of lithospheric deformation and upper mantle processes, and thus of the distribution of lateral resistivity inhomogeneities, in rift environments that is perpendicular to the direction of spreading. For the magnetotelluric method, a 2D transverse magnetic mode algorithm is most suitable for removing the distortion of MT soundings by such upper crustal structures and hence for assessing the resistivity of the deeper crust and upper mantle in extensional regimes. Equivalent 2D algorithms are not available for most controlled sources, although they are sorely needed.

An appropriately rigorous modeling technology has been applied to a collection of MT soundings in S.W. Utah and yielded an accurate profile of deep resistivity to depths exceeding 100 km. A feature required by the data is a low-resistivity (nominally 20 Ω-m) layer residing from about 35 to 65 km in the upper mantle beneath the Roosevelt Hot Springs. No low-resistivity layer in the middle to lower crust has been detected, however, nor do I think the case has yet been made on the basis of EM observations for such a layer to be widespread in the northern Basin and Range (cf. Eaton, 1982; Jiracek et al., 1983).

The present-day deep resistivity structure of southwestern Utah derives from the evolution of the northeastern Basin and Range through Late Cenozoic time. The low-resistivity layer interpreted in the upper mantle here is a manifestation of diapiric uprise and melting events occurring over an interval that extends to much greater depths than does the layer itself, perhaps in excess of 160 km. Both the resistivity structure and the timing and amplitude of extensional activity suggest that temperatures in the deep crust and uppermost mantle here exceed those which would be inferred from surface heat flow. Similar processes appear to be occurring in the northwestern Basin and Range, leaving central Nevada as a fairly quiescent region whose low-resistivity layering in the upper mantle, ironically, may be relatively pronounced. Unfortunately, deep resistivity surveys are lacking in the northern Basin and Range interior.

ACKNOWLEDGEMENTS

Thoughtful reviews and criticisms of this work by Drs. J.R. Bowman, D.S. Chapman, G.W. Hohmann, W.P. Nash, D.L. Nielson, W.T. Parry, W.R. Sill, C. M. Swift, Jr., and S.H. Ward are gratefully recognized. Technical assistance came from Sandra Bromley, Doris Cullen and Joan Pingree.

This work was supported by NSF contract EAR 8116602 and DOE/DGE contract DE-AC07-80ID12079.

REFERENCES

Allmendinger, R. W., Sharp, J. W., Von Tish, D., Serpa, L., Brown, L., Kaufman, S., Oliver, J., and Smith, R. B., 1983, Cenozoic and Mesozoic structure of the eastern Basin and Range province, Utah, from COCORP seismic-reflection data: Geology, 11, p. 532-536.

Best, M. G., McKee, E. H., and Damon, P. E., 1980, Space-time-composition patterns of Late Cenozoic mafic volcanism, southwestern Utah and adjoining areas: Am. J. Sci., 280, p. 1035-1050.

Bodell, J. M., and Chapman, D. S., 1982, Heat flow in the north-central Colorado Plateau: J. Geop. Res., 87(B4), p. 2869-2884.

Brace, W. F., 1971, Resistivity of saturated crustal rocks to 40 km based on laboratory measurements, In The Structure and Physical Properties of the Earth's Crust, ed. by J. G. Heacock, AGU Mono. 14, p. 243-256.

Burnham, C. W., 1979a, The importance of volatile constituents, In The Evolution of the Igneous Rocks: Fiftieth Anniversary Perspectives, ed. by H. S. Yoder, Jr., Princeton Univ. Press, p. 439-482.

_____, 1979b, Magmas and hydrothermal fluids, In Geochemistry of Hydrothermal Ore Deposits, ed. by H. L. Barnes, John Wiley and Sons, New York, p. 71-136.

Carter, J. A., and Cook, K. L., 1978, Regional gravity and aeromagnetic surveys of the Mineral Mountains and vicinity, Millard and Beaver Counties, Utah: ESL Report 77-11, 178 p.

Chapman, D. S., Clement, M. D., and Mase, C. W., 1981, Thermal regime of the Escalante Desert, Utah, with an analysis of the Newcastle geothermal system: J. Geop. Res. 86(B12), p. 11735-11746.

Christiansen, R. L., and McKee, E. H., 1978, Late Cenozoic volcanic and tectonic evolution of the Great Basin and Columbia intermontane region, In Cenozoic Tectonics and Regional Geophysics of the Western Cordillera, ed. by R. B. Smith and G. P. Eaton, GSA Mem. 152, p. 283-311.

Darot, M., and Gueguen, Y., 1981, High-temperature creep of forsterite single crystals: J. Geop. Res., 86(B7), p. 6219-6234.

Duba, A. G., Heard, H. C., and Schock, R. N., 1974, Electrical conductivity of olivine at high pressure and under controlled oxygen fugacity: J. Geop. Res., 79(11), p. 1667-1673.

Duba, A. G., and Heard, H. C., 1980, Effect of hydration on the electrical conductivity of olivine: EOS Transactions, 61(17), p. 404.

Eaton, G. P., 1982, The Basin and Range province: origin and tectonic significance: Ann. Rev. Earth Plan. Sci., 10, p. 409-440.

Gamble, T. D., Goubau, W. M., and Clarke, J., 1979, Magnetotellurics with a remote reference: Geophysics, 44(1), p. 53-68.

Gastil, R. G., 1979, A conceptual hypothesis for the relation of differing tectonic terranes to plutonic emplacement: Geology, 7, p. 542-544.

Gertson, R. C., and Smith, R. B., 1979, Interpretation of a seismic refraction profile across the Roosevelt Hot Springs, Utah and vicinity: ESL Report DOE/ID/78-1701.a.3, 116 p.

Gough, D. I., 1983, Electromagnetic geophysics and global tectonics: J. Geop. Res., 88(B4), p. 3367-3378.

Grant, F. S., and West, G. F., 1965, Interpretation Theory in Applied Geophysics: McGraw-Hill Book Company, Toronto, 584 p.

Hintze, L. F., 1973, Geologic history of Utah: Brigham Young Univ. Geology Studies, 20, pt. 3, 181 p.

_____, 1980, Geologic map of Utah: Utah Geological and Mineralogical Survey, Salt Lake City.

Jiracek, G. R., Mitchell, P. S., and Gustafson, E. P., 1983, Magnetotelluric results opposing magma origin of crustal conductors in the Rio Grande rift: Tectonophysics, 94, p. 299-326.

Jupp, D. L., and Vozoff, K., 1976, Discussion on "The magnetotelluric method in the exploration of sedimentary basins" by K. Vozoff: Geophysics, 41(2), p. 325-328.

Kariya, K. A., and Shankland, T. J., 1983, Interpretation of electrical conductivity of the lower crust: Geophysics, 48(1), p. 52-61.

Keller, G. V., 1971, Electrical studies of the crust and upper mantle, In the Structure and

Physical Properties of the Earth's Crust, ed. by J. G. Heacock, AGU Mono. 14, p. 107-125.

Keller, G. R., Braile, L. W., and Morgan, P., 1979, Crustal structure, geophysical models and contemporary tectonism of the Colorado Plateau: Tectonophysics, 61, p. 131-147.

Kirby, S. H., 1983, Rheology of the lithosphere: Reviews of Geophysics and Space Physics, 21(6), p. 1458-1487.

Lachenbruch, A. H., and Sass, J. H., 1978, Models of an extending lithosphere and heat flow in the Basin and Range province, In Cenozoic Tectonics and Regional Geophysics of the Western Cordillera, ed. by R. B. Smith and G. P. Eaton, GSA Mem. 152, p. 209-250.

Larsen, J. C., 1975, Low frequency (0.1-6.0 cpd) electromagnetic study of the deep mantle electrical conductivity beneath the Hawaiian Islands: Geop. J. Roy. Ast. Soc., 43, p. 17-46.

_____, 1981, A new technique for layered earth magnetotelluric inversion: Geophysics, 46(9), p. 1247-1257.

Lienert, B. R., 1979, Crustal electrical conductivities along the eastern flank of the Sierra Nevadas: Geophysics, 44(11), p. 1830-1845.

Lienert, B. R., and Bennett, D. J., 1977, High electrical conductivities in the lower crust of the northwestern Basin and Range: an application of inverse theory to a controlled-source deep-magnetic-sounding experiment, In The Earth's Crust, ed. by J. G. Heacock, AGU Mono. 20, p. 531-552.

Luedke, R. G., and Smith, R. L., 1978a, Map showing distribution, composition, and age of Late Cenozoic volcanic centers in Arizona and New Mexico, U.S.G.S. Miscellaneous Investigations Series, Map 1-1091-A.

_____, 1978b, Map showing distribution, composition, and age of Late Cenozoic volcanic centers in Colorado, Utah, and southwestern Wyoming, U.S.G.S. Miscellaneous Investigations Series, Map 1-1091-B.

_____, 1981, Map showing distribution, composition, and age of Late Cenozoic volcanic centers in California and Nevada, U.S.G.S. Miscellaneous Investigation Series, Map 1-1091-C.

Madden, T. R., 1971, The resolving power of geoelectric measurements for delineating resistive zones within the crust, In The Structure and Physical Properties of the Earth's Crust, ed. by J. G. Heacock, AGU Mono. 14, p. 95-105.

Mysen, B. O., and Kushiro, I., 1977, Compositional variations of coexisting phases with degree of melting of peridotite in the upper mantle: Am. Min., 62, p. 843-865.

Nash, W. P., 1983, Silicic volcanism along the eastern margin of the Basin and Range province: Utah and Idaho: GSA Abstracts with Programs, p. 402.

Oxburgh, E. R., 1980, Heat flow and magma genesis, In Physics of Magmatic Processes, ed. by R. B. Hargraves, Princeton Univ. Press, p. 161-200.

Padovani, E. R., Hall, J., and Simmons, G., 1982, Constraints on crustal hydration below the Colorado Plateau from V_p measurements on crustal xenoliths: Tectonophysics, 84, p. 313-328.

Parker, R. L., and Whaler, K. A., 1981, Numerical methods for establishing solutions to the inverse problem of electromagnetic induction: J. Geop. Res., 86(B10), p. 9574-9584.

Petrick, W. R., Pelton, W. H., and Ward, S. H., 1977, Ridge regression inversion applied to crustal resistivity sounding data from South Africa: Geophysics, 42(5), p. 995-1005.

Petrick, W. R., Sill, W. R., and Ward, S. H., 1981, Three-dimensional resistivity inversion using alpha centers: Geophysics, 46(8), p. 1148-1162.

Porath, H., 1971, Magnetic variation anomalies and seismic low-velocity zone in the western United States: J. Geop. Res., 76(11), p. 2643-2648.

Porath, H., and Gough, D. I., 1971, Mantle conductive structures in the western United States from magnetometer array studies: Geop. J. Roy. Ast. Soc., 22, p. 261-275.

Porath, H., Oldenburg, D. W., and Gough, D. I., 1970, Separation of magnetic variation fields and conductive structures in the western United States: Geop. J. Roy. Ast. Soc., 19, p. 237-260.

Priestley, K., and Brune, J. N., 1978, Surface waves and the structure of the Great Basin of Nevada and western Utah: J. Geop. Res., 83 (B5), p. 2265-2272.

Priestley, K., Orcutt, J. A., and Brune, J. N., 1980, Higher-mode surface waves and structure of the Great Basin of Nevada and western Utah: J. Geop. Res., 85(B12), p. 7166-7174.

Proffett, J. M., Jr., 1977, Cenozoic geology of the Yerrington district, Nevada, and implications for the nature and origin of Basin and Range faulting: GSA Bull., 88, p. 247-266.

Rai, C. S., and Manghnani, M. H., 1978, Electrical conductivity of basalts to 1550°C, In Proceedings of Chapman Conference on Partial Melting in the Earth's Upper Mantle, ed. by H. J. B. Dick, Oreg. Dept. Geol. Min. Ind., Bull. 96, p. 219-232.

Reitzel, J. S., Gough, D. I., Porath, H., and Anderson, C. W., III, 1970, Geomagnetic deep soundings and upper mantle structure in the western United States: Geop. J. Roy. Ast. Soc., 19, p. 213-235.

Rijo, L., 1977, Modeling of electric and electromagnetic data: Ph.D. Thesis, Dept. of Geology and Geophysics, Univ. of Utah.

Ross, H. P., Nielson, D. L., and Moore, J. N., 1982, Roosevelt Hot Springs geothermal system, Utah - case study: Am. Assoc. Petr. Geol. Bull., 66(7), p. 879-902.

Rowley, P. D., Steven, T. A., Anderson, J. J., and Cunningham, C. G., 1979, Cenozoic stratigraphic and structural framework of southwestern Utah: U.S.G.S Professional Paper 1149, 22 p.

Sass, J. H., Blackwell, D. D., Chapman, D. S., Costain, J. K., Decker, E. R., Lawver, L. A., and Swanberg, C. A., 1981, Heat flow from the crust of the United States, in Physical Properties of Rocks and Minerals, ed. by Y. S. Touloukian and C. Y. Ho, McGraw-Hill/CINDAS Data Series on Material Properties, II-2, New York, p. 503-548.

Schmucker, U., 1970, Anomalies of geomagnetic variations in the southwestern United States, Bull. Scripps Inst. Oceanography, 13, 165 p.

Smith, R. B., 1978, Seismicity, crustal structure and intraplate tectonics of the interior of the western Cordillera, In Cenozoic Tectonics and Regional Geophysics of the Western Cordillera, ed. by R. B. Smith and G. P. Eaton, GSA Mem. 152, p. 111-144.

Spear, F. S., and Silverstone, J., 1983, Water exsolution from quartz: implications for the generation of retrograde metamorphic fluids: Geology, 11(2), p. 82-85.

Spera, F. J., 1980, Aspects of magma transport, In Physics of Magmatic Processes, ed. by R. B. Hargraves, Princeton Univ. Press, p. 265-324.

Stanley, W. D., Wahl, R. R., and Rosenbraum, J. G., 1976, A magnetotelluric study of the Stillwater-Soda Lakes, Nevada, geothermal area: U.S.G.S. Open-File Report 76-80, 38 p.

Stanley, W. D., Boehl, J. E., Bostick, F. X., Jr., and Smith, H. W., 1977, Geothermal significance of magnetotelluric soundings in the Snake River Plain - Yellowstone region: J. Geop. Res., 82(17), p. 2501-2514.

Stewart, J. H., 1978, Basin and Range structure in western North America: a review, In Cenozoic Tectonics and Regional Geophysics of the Western Cordillera, ed. by R. B. Smith and G. P. Eaton, GSA Mem. 152, p. 1-31.

_____, 1980, Geology of Nevada: Nevada Bureau of Mines and Geology Special Pub. 4, 136 p.

Stodt, J. A., 1978, Documentation of a finite element program for solution of geophysical problems governed by the inhomogeneous 2-D scalar Helmholtz equation: NSF Program Listing and Documentation, ESL, 66 p.

_____, 1983, Bias removal for conventional magnetotelluric data: ESL report, in press, Salt Lake City.

Stolper, E., Walker, D., Hager, B. H., and Hays, J. F., 1981, Melt segregation from partially molten source regions: the importance of melt density and source region size: J. Geop. Res., 86(B7), p. 6261-6272.

Swift, C. M., 1967, A magnetotelluric investigation of an electrical conductivity anomaly in the southwestern United States: Ph.D. thesis, Massachusetts Institute of Technology, 211 p.

Thompson, G. A., and Zoback, M. L., 1979, Regional geophysics of the Colorado Plateau: Tectonophysics, 61, p. 149-181.

Ting, S. C., and Hohmann, G. W., 1981, Integral equation modeling of three-dimensional magnetotelluric response: Geophysics, 46(2), p. 182-197.

Towle, J. N., 1980, Observations of a direct current concentration on the eastern Sierran front: evidence for shallow crustal conductors on the eastern Sierran front and beneath the Coso Range: J. Geop. Res., 85(B5), p. 2484-2490.

Turcotte, D. L., 1982, Magma migration: Ann. Rev. Earth Plan. Sci., 10, p. 397-408.

Vozoff, K., 1972, The magnetotelluric method in the exploration of sedimentary basins: Geophysics, 37(1), p. 98-141.

Waff, H. S., and Bulau, J. R., 1979, Equilibrium fluid distribution in an ultramafic partial melt under hydrostatic stress conditions: J. Geop. Res., 84(B11), p. 6109-6114.

Wannamaker, P. E., Hohmann, G. W., and Ward, S. H., 1983, Magnetotelluric responses of three-dimensional bodies in layered earths: submitted to Geophysics.

Ward, S. H., 1967, Electromagnetic theory for geophysical application, In Mining Geophysics, II, Society of Exploration Geophysics, Tulsa, p. 10-196.

Ward, S. H., 1983, Controlled source electrical methods for deep exploration: Geop. Surv., in press.

Ward, S. H., Parry, W. T., Nash, W. P., Sill, W. R., Cook, K. L., Smith, R. B., Chapman, D. S., Brown, F. H., Whelan, J. A., and Bowman, J. R., 1978, A summary of the geology, geochemistry and geophysics of the Roosevelt Hot Springs thermal area, Utah: Geophysics, 43(7), p. 1515-1542.

Weinstock, H., and Overton, W. C., Jr., 1981, SQUID applications in geophysics: SEG, Tulsa, 208 p.

Wernicke, B., and Burchfiel, B.C., 1982, Modes of extensional tectonics: J. Struc. Geol., 4(2), p. 105-115.

Williams, L. A. J., 1982, Physical aspects of magmatism in continental rifts, In Continental and Oceanic Rifts, ed. by G. Palmasson, AGU Geodynamics Series, 8, p. 193-222.

Wilt, M. J., Goldstein, N. E., Haught, J. R., and Morrison, H. F., 1982, Deep electromagnetic soundings in central Nevada: Expanded abstract of paper presented at the 52nd annual meeting of the SEG, Dallas, TX.

Winkler, H. C. F., 1979, Petrogenesis of metamorphic rocks: Fifth ed., Springer-Verlag, New York, 348 p.

Word, D. R., Smith, H. W., and Bostick, F. X., Jr., 1971, Crustal investigations by the magnetotelluric impedance method, In The Structure and Physical Properties of the Earth's Crust, ed. by J. G. Heacock, AGU Mono. 14, p. 145-167.

Wyllie, P. J., 1979, Petrogenesis and the physics of the earth, In The Evolution of the Igenous Rocks: Fiftieth Anniversary Perspectives, ed. by H. S. Yoder, Jr., Princeton Univ. Press, p. 483-520.

Yoder, H. S., Jr., 1976, Generation of basaltic magma: National Academy of Sciences, Washington, 265 p.

Zoback, M. L., Anderson, R. E., and Thompson, G. A., 1981, Cenozoic evolution of the state of stress and style of tectonism of the Basin and Range province of the western United States: Phil. Trans. Roy. Soc. Lond., A 300, p. 407-434.